

Supplementary Information for

**Reversible Solid-to-Liquid Phase Transition of
Coordination Polymer Crystals**

Daiki Umeyama¹, Satoshi Horike^{1,2*}, Munehiro Inukai³, Tomoya Itakura⁴, Susumu Kitagawa^{1,3*}

¹Department of Synthetic Chemistry and Biological Chemistry, Graduate School of Engineering, Kyoto University, Katsura, Nishikyo-ku, Kyoto 615-8510, Japan.

²PRESTO, Japan Science and Technology Agency, 4-1-8 Honcho, Kawaguchi, Saitama 332-0012, Japan.

³Institute for Integrated Cell-Material Sciences (WPI-iCeMS), Kyoto University, Yoshida, Sakyo-ku, Kyoto 606-8501, Japan.

⁴DENSO Corporation, 1-1 Showa-cho, Kariya, Aichi 448-8661, Japan.

*To whom correspondence should be addressed. Email: horike@sbchem.kyoto-u.ac.jp (S.H);
kitagawa@icems.kyoto-u.ac.jp (S.K.)

General Methods

The single crystal X-ray diffraction measurement were performed at 223 K with a Rigaku AFC10 diffractometer with Rigaku Saturn Kappa CCD system equipped with a MicroMax-007 HF/VariMax rotating-anode X-ray generator with confocal monochromated MoK α radiation. The data were processed by a direct method (SIR97) and refined by full-matrix least-squares refinement using the SHELXL-97 computer program.

The powder X-ray diffractions (PXRD) were collected on a Rigaku RINT 2200 Ultima diffractometer with Cu anode.

The solid state ^{31}P MAS was recorded on a Bruker ADVANCE 400 MHz spectrometer. The spectrum for **1** was measured with dipolar-decoupling MAS (5 kHz), for **1'** with dipolar-decoupling MAS (1 kHz), for **1''** with cross-polarization MAS (10 kHz).

Variable-temperature viscoelastic measurement was performed by using a rotational parallel-plate rheometer (Rheosol-G5000, UBM Co., Ltd.) under dry N $_2$ flow with applying oscillatory strain of 1 Hz. The sample-holding gap was set to 1.0 mm.

The infra-red (IR) Spectroscopy was obtained using a Nicolet ID5 ATR with a diamond sample stage operating at ambient temperature.

The differential scanning calorimetry (DSC) was carried out with a DSC6220 (SII Nano Technology Inc.) at the heating rate of 10 K min $^{-1}$. The extrapolated onset temperatures was determined by using a software Muse Standard Analysis (version 6.2; SII Nano Technology Inc.).

Table S1. Summary of characteristics of melting CPs.

Compound	Behaviour when heated	Melting point	Structural dimension	Array around metal ion
[Zn(HPO ₄)(H ₂ PO ₄) ₂] \cdot 2H ₂ Im (1)	melt	154 °C	1D	<i>T_d</i>
[Zn(H ₂ PO ₄) ₂ (HTr) ₂] (2)	melt	184 °C	2D	<i>O_h</i>
[Zn ₃ (H ₂ PO ₄) ₆ (H ₂ O) ₃] \cdot HBim (3)	melt	164 °C	1D	<i>O_h</i>
[Zn ₃ (H ₂ PO ₄) ₆ (H ₂ O) ₃] \cdot H(2-MeBim) (4)	melt	97 °C	1D	<i>O_h</i>
[Zn ₃ (H ₂ PO ₄) ₆ (H ₂ O) ₃] \cdot H(2-ClBim) (5)	solidify	n/a	1D	<i>O_h</i>
[Co ₃ (H ₂ PO ₄) ₆ (H ₂ O) ₃] \cdot HBim (6)	decompose	n/a	1D	<i>O_h</i>

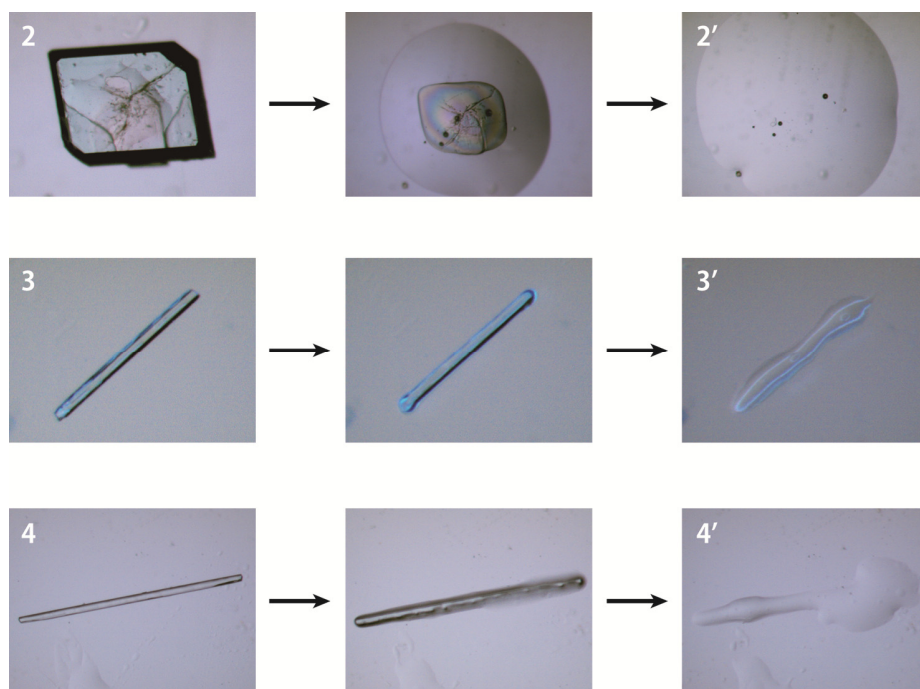


Figure S1. Microscopy images of 2, 3 and 4 during solid-to-liquid phase transition.

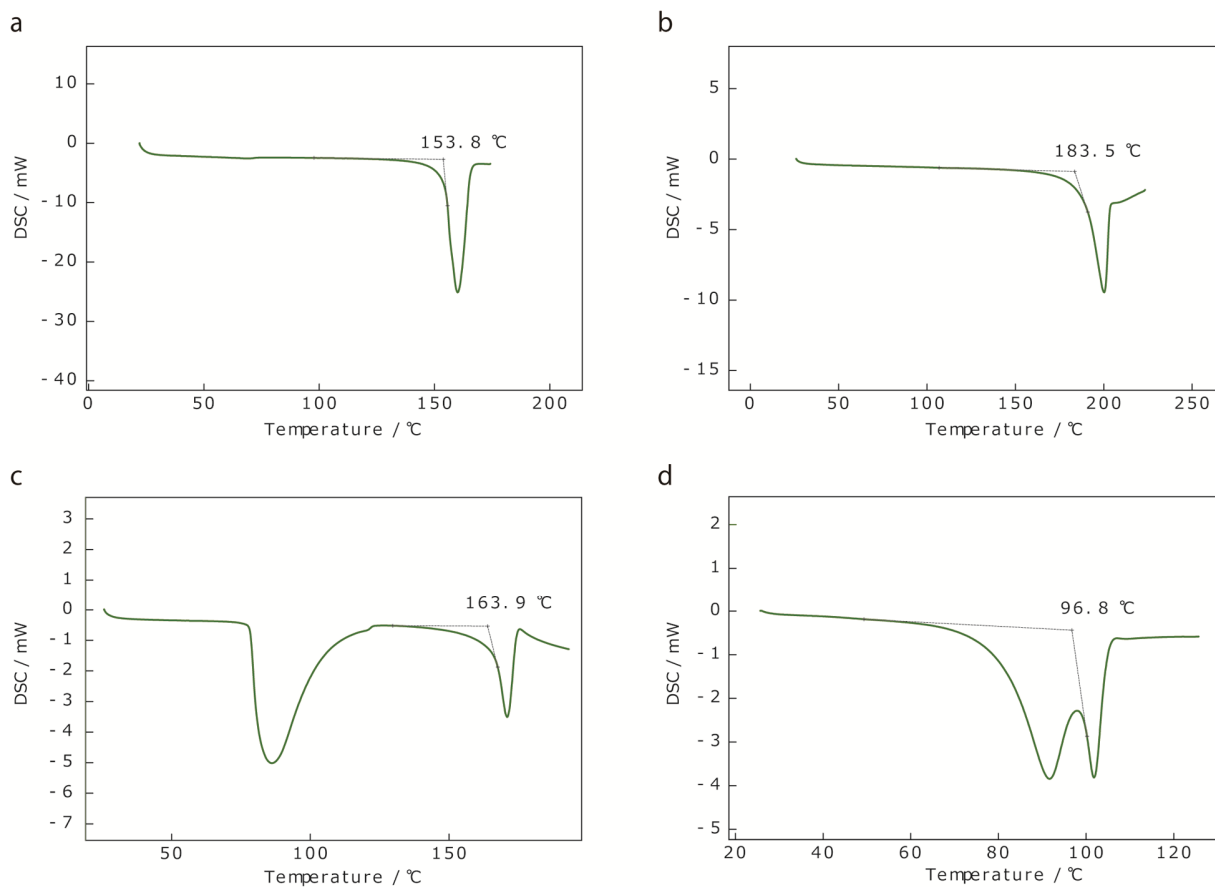


Figure S2. DSC curves of (a) 1, (b) 2, (c) 3 and (d) 4. Each melting point was determined as extrapolated onset temperature of the endothermic event. The broad peaks prior to the melting points observed for **3** and **4** originate from the dehydration of these compounds.

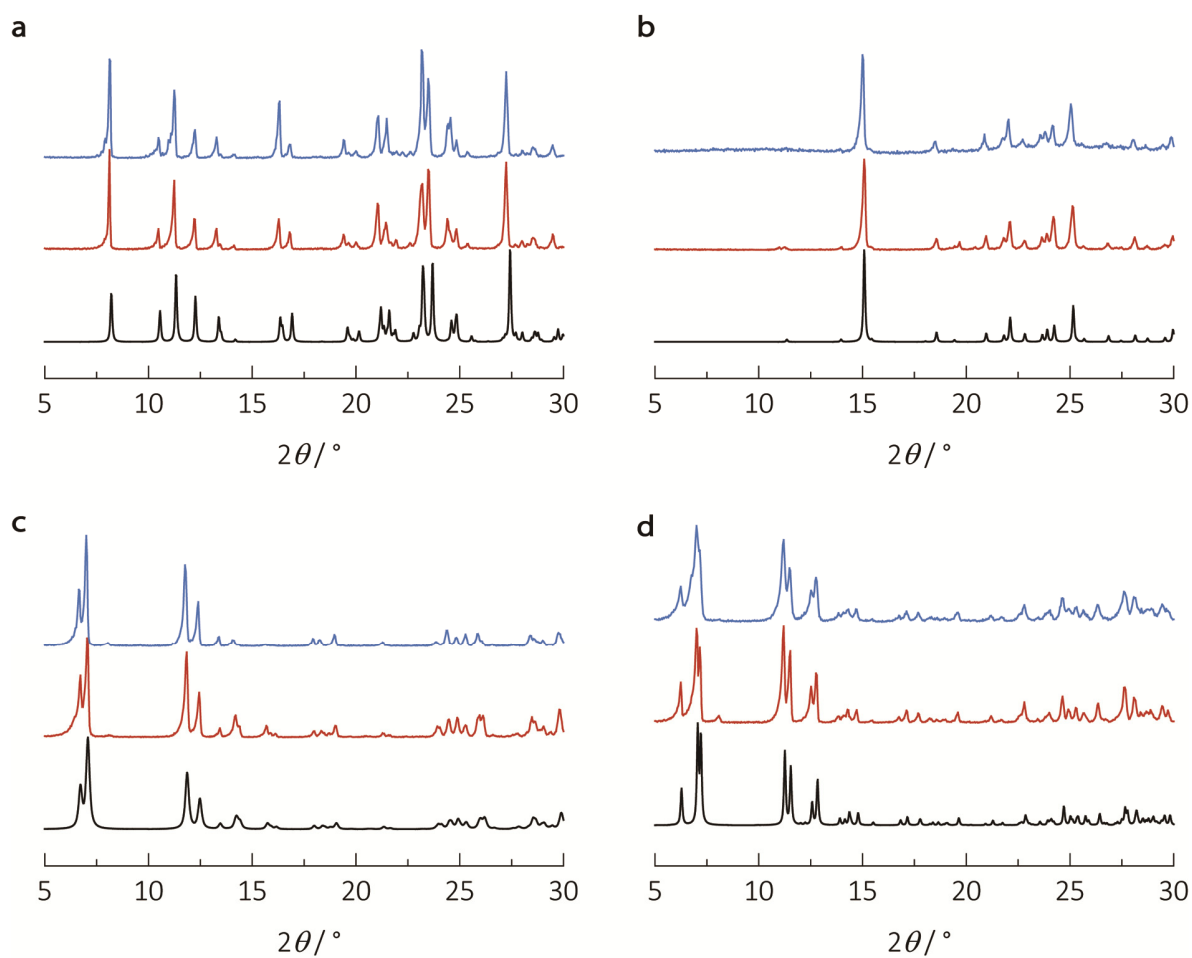


Figure S3. PXRD patterns of as synthesized and recrystallized 1, 2, 3 and 4. (a) 1, (b) 2, (c) 3, and (d) 4. Simulated patterns from the crystal structures are shown in black, patterns of as synthesized samples are in red, and recrystallized samples are in blue.

Table S2. Crystallographic data and structural refinement summary for 4.

Asymmetric unit	C ₈ H ₇ N ₂ O ₂₈ P ₆ Zn ₃
Crystal system	triclinic
Space group	<i>P</i> -1 (#2)
<i>a</i> (Å)	13.8557(17)
<i>b</i> (Å)	15.1778(19)
<i>c</i> (Å)	16.237(2)
α (°)	102.734(5)
β (°)	115.096(4)
γ (°)	95.621(7)
<i>V</i> (Å ³)	2944.4(7)
<i>Z</i>	2
Temperature (K)	213
No. of reflections measured	20426
No. of independent reflections	12729
<i>R</i> _{int}	0.0249
Final <i>R</i> ₁ (<i>I</i> > 2σ(<i>I</i>)) ^a	0.0455
Final <i>wR</i> (<i>F</i> ²) (<i>I</i> > 2σ(<i>I</i>)) ^b	0.1412
Final <i>R</i> ₁ (all data)	0.0641
Final <i>wR</i> (<i>F</i> ²) (all data)	0.1524
Goodness of fit (GOF) on <i>F</i> ²	0.827

^a $R_1 = (|F_o| - |F_c|)/|F_o|$

^b $wR_2 = [w(F_o^2 - F_c^2)/w(F_o^2)^2]^{1/2}$

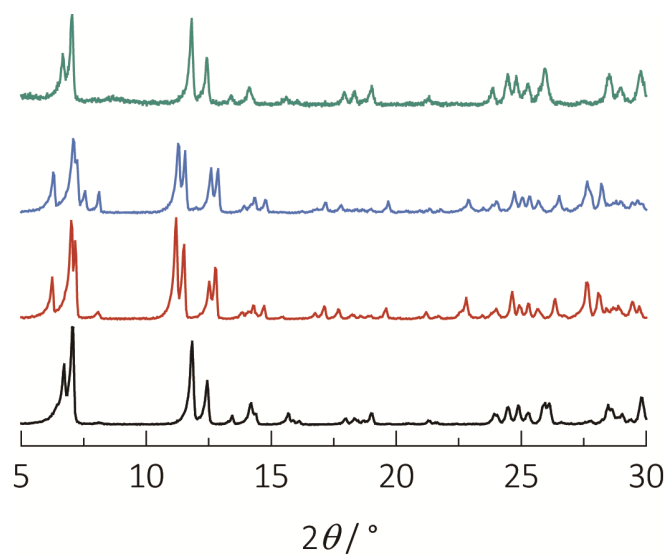


Figure S4. PXRD patterns of as synthesized 3 (black), 4 (red), 5 (blue) and 6 (green).

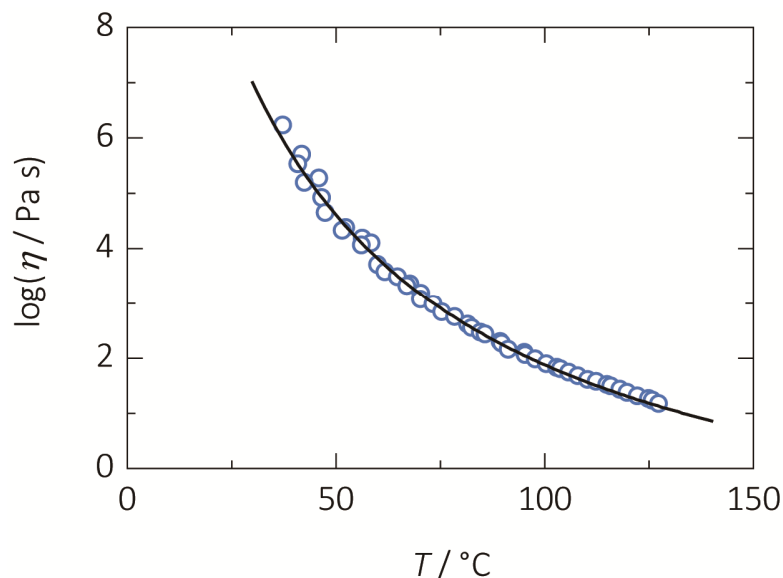


Figure S5. Viscosity of 1'. Experimental values (blue circle) and fit by Vogel equation (black line) of $\log\eta = A + B / (T - C)$; $A = -2.41$, $B = 553$ °C, $C = -28.7$ °C.

The viscosity of **1'** deduced from shear modulus continuously changes from 10^6 Pa s to 10^1 Pa s through 35 to 130 °C with Vogel type temperature dependency, which is typical to ionic liquids¹ (Fig S4). The viscosity of **1'** is more than 100 times higher than that of partially condensed phosphoric acid.² This is rationalized by the fact that **1'** has ionic interactions between zinc, phosphate and imidazolium ions, in addition to coordination-bond and hydrogen-bond interaction. The viscosity of **1''** below 35 °C is too high to be measured, which represents the glassy state of **1''** where a stronger interaction such as coordination bond is supposed to be present in a more rigid form.

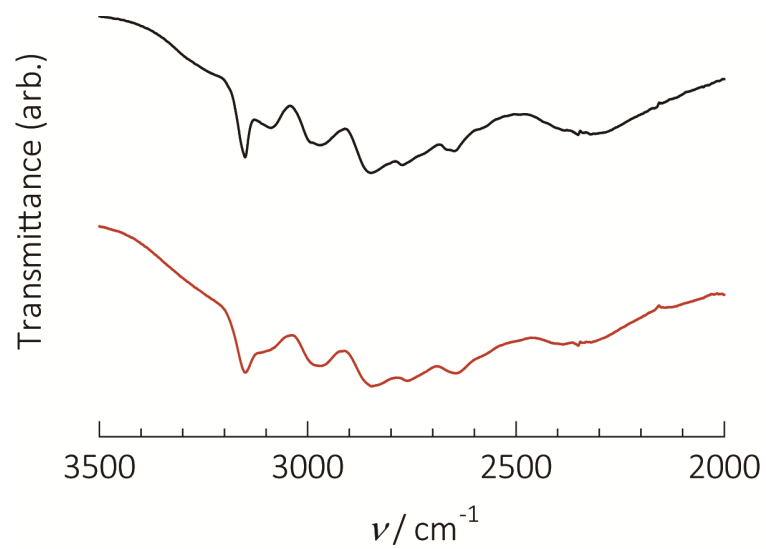


Figure S6. IR spectra of 1 (black) and 1'' (red).

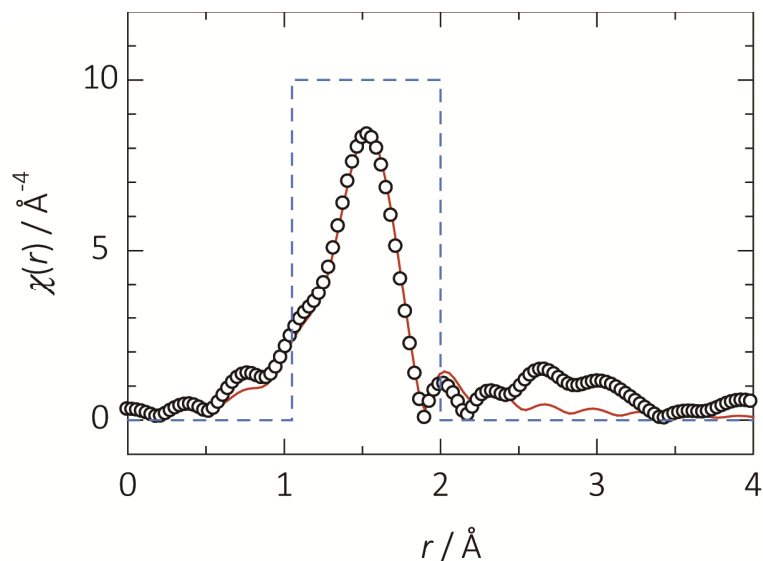


Figure S7. RDF of 1'' (black circle) and fitting (red line). The fitting range is shown with blue dashed line.

The following equation was used to calculate and fit RFD of 1'':

$$\chi(k) = S_0^2 \sum \frac{N_j f_j(k) \exp[-2k^2 \sigma_j^2]}{kr_j^2} \sin[2k_j r_j + \delta(k)]$$

where r is distance from the target to neighboring atom, N is coordination number of the neighboring atom, and σ^2 is Debye-Waller factor. The photoelectron wavenumber k is given as $k = \sqrt{2m(E - E_0)/\hbar^2}$, $f(k)$ is the scattering amplitude, and $\delta(k)$ is the phase shift. S_0 , amplitude reduction factor, was empirically determined from EXAFS of **1** (crystalline state) as 1.03(12). EXAFS spectrum of 1'' was fitted in r range from 1.05 to 2.00 Å. The final values of these parameters are summarised in Table S2.

Table S3. Parameters refined by fitting the EXAFS spectrum of 1''.

Shell	N	$r / \text{\AA}$	$\sigma^2 / \text{\AA}^2$	E_0 / eV	R -factor
Zn–O	4.0(2)	1.94(3)	0.0059(4)	3.9(7)	0.0011

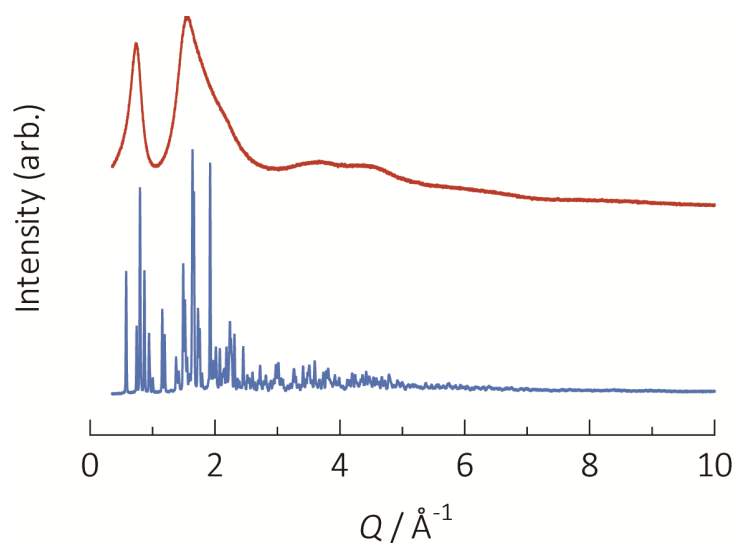
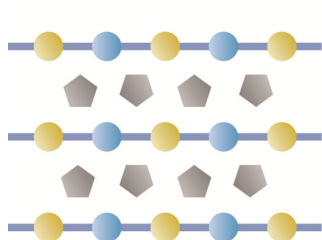
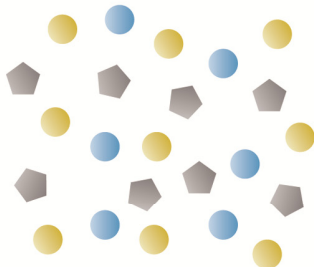


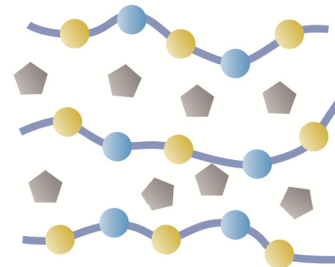
Figure S8. X-ray total scattering profile of 1 (blue) and 1'' (red).



1 (crystal)



1' (melt)



1'' (glass)

● zinc ion ● phosphate ◡ imidazolium

Figure S9. Schematic illustration of the structures of 1, 1' and 1''.

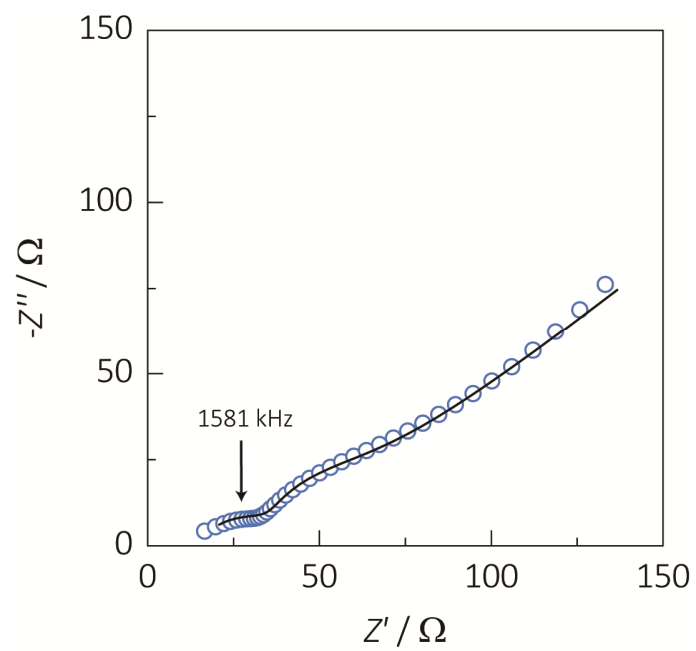


Figure S10. Nyquist plot of the thin film of 1 at 120 °C. Blue circles are experimental data and black line is simulated values from equivalent circuit.

References

- (1) Bruce, E. P.; John, M. P.; John, P. O. C. *Properties of Gases and Liquids, Fifth Edition*; McGraw-Hill, **2001**.
- (2) Wang, Y. Y.; Lane, N. A.; Sun, C. N.; Fan, F.; Zawodzinski, T. A.; Sokolov, A. P. *J. Phys. Chem. B* **2013**, *117*, 8003.